NeuroImage 227 (2021) 117676

Contents lists available at ScienceDirect

NeuroImage

journal homepage: www.elsevier.com/locate/neuroimage

Time between milestone events in the Alzheimer's disease amyloid cascade

Philip S. Insel[a,b,*], Michael C. Donohue[c], David Berron[a], Oskar Hansson[a,d], Niklas Mattsson-Carlgren[a,e,f,*]

[a] Clinical Memory Research Unit, Department of Clinical Sciences Malmö, Lund University, Sweden
[b] Department of Psychiatry and Behavioral Sciences, University of California, San Francisco, CA, United States
[c] Alzheimer's Therapeutic Research Institute, Keck School of Medicine, University of Southern California, San Diego, CA, United States
[d] Memory Clinic, Skåne University Hospital, Malmö, Sweden
[e] Department of Neurology, Skåne University Hospital, Lund, Sweden
[f] Wallenberg Center for Molecular Medicine, Lund University, Lund, Sweden

ARTICLE INFO

Keywords:
Alzheimer's disease
β-amyloid
Tau PET
Cognition

ABSTRACT

Objective: Estimate the time-course of the spread of key pathological markers and the onset of cognitive dysfunction in Alzheimer's disease.

Methods: In a cohort of 335 older adults, ranging in cognitive functioning, we estimated the time of initial changes of Aβ, tau, and decreases in cognition with respect to the time of Aβ-positivity.

Results: Small effect sizes of change in CSF Aβ42 and regional Aβ PET were estimated to occur several decades before Aβ-positivity. Increases in CSF tau occurred 7–8 years before Aβ-positivity. Temporoparietal tau PET showed increases 4–5 years before Aβ-positivity. Subtle cognitive dysfunction was observed 4–6 years before Aβ-positivity.

Conclusions:: Increases in tau and cognitive dysfunction occur years before commonly used thresholds for Aβ-positivity. Explicit estimates of the time for these events provide a clearer picture of the time-course of the amyloid cascade and identify potential windows for specific treatments.

Introduction

Disconcerting clinical trial results for the treatment of Alzheimer's disease (AD) have led to a shift toward earlier intervention, focusing on the early clinical or presymptomatic phases, when biomarkers are needed to identify the disease. The amyloid cascade (Hardy and Selkoe, 2002) is thought to start with elevated levels of two key amyloids in the brain, β-amyloid (Aβ) and tau, and end with severe cognitive and functional impairment (Jack et al., 2010). Growing evidence suggests that an early sign that the cascade has begun is change in cerebrospinal fluid (CSF) Aβ, potentially detectable prior to significant Aβ deposition in the brain as measured by positron emission tomography (PET) (Palmqvist et al., 2016). This accumulation of Aβ has been suggested to be followed by increases in CSF tau and the spread of tau pathology beyond the temporal lobe (Braak and Braak, 1991; Schöll et al., 2016). The build-up and spread of these two brain pathologies is paralleled by gradual cognitive and functional decline (Zetterberg and Mattsson, 2014).

Previous neuropathological and biomarker data suggest that the overall time-course of AD is several decades (Li et al., 2017; Villemagne et al., 2013). In autosomal dominant AD, the estimated years to clinical onset has been used to estimate the time-course of different biomarkers in AD (Bateman et al., 2012). However, the time-course of the spread of Aβ and tau and the onset of clinical symptoms in sporadic AD is unknown. With repeated measures of Aβ over time, the level and rate of change with respect to the key initiating AD pathology may offer a measure of disease progression in sporadic AD. The duration of amyloid positivity (chronicity) has been shown to be associated with increased tau pathology and faster cognitive decline and valuable in explaining heterogeneity in early disease progression (Koscik et al., 2020). With level and change information, the time from the threshold for significant Aβ pathology can be estimated within individuals, providing the temporal disease progression information important for evaluating biomarker trajectories. Without longitudinal information, cross-sectional studies frequently categorize subjects into two groups – those below a threshold for significant pathology and those above, where subjects just below the threshold who will cross over within months are considered pathologically equivalent to subjects who will not cross over for decades. By incorporating longitudinal information, disease progression with respect to Aβ pathology can be represented to reflect its continuous nature, resulting in a more

* Corresponding authors at: Clinical Memory Research Unit, Department of Clinical Sciences Malmö, Lund University, Sweden.
E-mail addresses: philip.insel@med.lu.se (P.S. Insel), niklas.mattsson-carlgren@med.lu.se (N. Mattsson-Carlgren).

https://doi.org/10.1016/j.neuroimage.2020.117676
Received 28 July 2020; Received in revised form 29 October 2020; Accepted 15 December 2020
Available online 24 December 2020

powerful way to model the relationship between Aβ and downstream processes.

The aims of this study were to demonstrate the utility and predictive ability of the time-from-Aβ-positivity (TFAβ+) formulation and to evaluate the relationships between TFAβ+ and downstream biomarker and cognitive responses in order to estimate the time of the earliest signs of progression in sporadic AD. Using serial ^{18}F-florbetapir (Aβ) PET measurements, rates of change of Aβ were estimated and used to calculate the time-from-threshold for each subject. These subject-specific estimates of the proximity to the threshold for Aβ-positivity (Aβ+) were then used to model the trajectories and temporal ordering of other key markers in AD including CSF Aβ42, regional Aβ PET, several measures of tau including CSF phosphorylated (P-tau) and total tau (T-tau), regional ^{18}F-flortaucipir (AV-1451) tau PET, and cognition. Estimates of the time and ordering of these pathophysiological changes may facilitate the design of future prevention trials and identify a window for early treatment.

Materials and methods

Standard protocol approvals, registrations, and patient consents

This study was approved by the Institutional Review Boards of all of the participating institutions. Informed written consent was obtained from all participants at each site.

Data availability

All data is publicly available (http://adni.loni.usc.edu/). R code is available on Github.

Participants

Data were obtained from the Alzheimer's Disease Neuroimaging Initiative (ADNI) database (http://adni.loni.usc.edu/, www.adni-info.org) on 1/21/2020. An initial analysis was done on ADNI participants with available Aβ PET data (in N = 962 Aβ- cognitively unimpaired (CU-), Aβ+ cognitively unimpaired (CU+), Aβ+ MCI and Aβ+ AD), to facilitate the estimation of TFAβ+, though not all 962 were included in the analysis of the main outcomes. Participants were classified as cognitively unimpaired if they had an MMSE score of 24–30, CDR score of 0, no memory complaint, and a Logical Memory II subscale of the Wechsler Memory Scale-Revised score $\geq$ 9 for 16 years of education, $\geq$ 5 for 8–15 years of education, and $\geq$ 3 for 0–7 years of education. Participants were classified as MCI if they had an MMSE score of 24–30, a CDR score of 0.5 as well as a memory box score of 0.5, and a Logical Memory II score $\leq$ 8 for 16 years of education, $\leq$ 4 for 8–15 years of education, and $\leq$ 2 for 0–7 years of education. Subjects were classified as having AD dementia if they had a memory complaint, met the same criteria for Logical Memory as the MCI group, had a CDR score of 0.5 or 1, and met the National Institute of Neurological and Communicative Disorders and Stroke–Alzheimer's Disease and Related Disorders Association criteria for probable AD. The population in the primary analyses of PET and cognitive outcomes only included ADNI participants with available measurements of Aβ and tau PET and cognition. Of these, all cognitively unimpaired (CU- and CU+), prodromal AD (Aβ+ MCI) and Aβ+ AD dementia participants were included in the analysis, where Aβ-positivity was defined using a previously established threshold (Standardized Uptake Value Ratio, SUVR = 1.10) (Joshi et al., 2012). Aβ- MCI (N = 224, including Aβ- CU to MCI progressors) and Aβ- "AD dementia" subjects (N = 51, including Aβ- MCI to AD dementia progressors; we consider these to be misdiagnosed, because we assume AD requires Aβ+) were not included in the main analysis given our aim to model head to head comparisons of initial biomarker and cognitive changes of individuals on the AD continuum and not other diseases. In order to estimate the time of emerging cognitive decline associated with increasing Aβ, those with cognitive impairment, but low levels of Aβ were excluded. MCI and AD participants were considered Aβ- if their SUVR remained below the threshold at all scans during follow-up. Visualizations of their biomarker data are included for comparison in Figs. 2–4 (see Figure legends). Additional description is included in the statistical analysis section.

Cerebrospinal fluid biomarker concentrations

Cerebrospinal fluid (CSF) samples were collected at baseline by lumbar puncture in a subsample (N = 185). CSF Aβ42, total tau (T-tau) and phosphorylated tau (P-tau) were measured by an xMAP assay (INNOBIA AlzBio3, Ghent, Belgium, Fujirebio), as described previously (Olsson et al., 2005; Shaw et al., 2009).

PET imaging

Methods to acquire and process Aβ (18F-florbetapir) PET image data were described previously (Jagust et al., 2015; Landau et al., 2012). Briefly, florbetapir image data were acquired 50–70 min postinjection, and images were averaged, spatially aligned, interpolated to a standard voxel size, and smoothed to a common resolution of 8 mm full width at half maximum. We used an a priori defined threshold for Aβ-positivity (SUVR=1.1) (ADNI, 2012; Joshi et al., 2012) applied to the ratio of the average of the four target regions (temporal, cingulate, frontal, and parietal lobes) and the cerebellum, in the estimation of time-from-Aβ-positivity, described in detail below. In a second part of the analysis, five Aβ PET ROI outcomes were considered (Landau and Jagust, 2015; Mormino et al., 2009), (1) the temporal lobe (middle and superior temporal lobe), (2) the parietal lobe (precuneus, supramarginal, inferior and superior parietal lobe), (3) the cingulate gyrus (isthmus, posterior, caudal and rostral anterior cingulate), (4) the frontal lobe (pars opercularis, pars triangularis, pars orbitalis, caudal/rostral middle frontal, medial/lateral orbitofrontal, frontal pole, and superior frontal lobe), and (5) a composite of regions thought to be early in accumulating Aβ (precuneus and posterior cingulate) (Palmqvist et al., 2017). These ROIs comprise the regions included in the global composite, grouped into individual lobes plus an additional early ROI. 18F-florbetapir ROIs were expressed as SUVRs with a cerebellar reference region.

Methods to acquire and process tau (18F-flortaucipir) PET image data were described previously (Maass et al., 2017). Six tau ROI outcomes, corrected for partial-volume, were considered: (1) the medial temporal lobe (MTL) (amygdala, entorhinal and parahippocampal cortex; from Braak stage I and III), (2) the lateral temporal lobe (LTL) (inferior/middle/superior temporal lobe, banks of the superior temporal sulcus, transverse temporal lobe, temporal pole; from Braak stage IV and V), (3) the medial parietal lobe (MPL) (isthmus cingulate, precuneus; from Braak stage IV and V), (4) the lateral parietal lobe (LPL) (inferior/superior parietal lobe, supramarginal; from Braak stage V), (5) frontal lobe (pars, orbitofrontal and middle/superior frontal lobe; from Braak stage V), and (6) the occipital lobe (cuneus, lingual, pericalcarine, and lateral occipital lobe; from Braak stage III, V, and VI). 18F-flortaucipir ROIs were expressed as SUVRs with an inferior cerebellar gray matter reference region. Scanner type and site were evaluated for their association with PET outcomes through covariate adjustment. Full details of PET acquisition and analysis can be found at http://adni.loni.usc.edu/methods/.

Cognition

Cognitive measures assessed included the Mini-Mental State Examination (MMSE) as a measure of global cognition, and the Preclinical Alzheimer's Cognitive Composite (PACC), as a measure of early AD-related cognitive changes. The PACC comprised the MMSE, the Logical Memory Delayed Word Recall from the Wechsler Memory Scale, the Alzheimer's Disease Assessment Scale—Cognitive Subscale Delayed Word Recall, and the Trail Making Test part B (reversed such

that high scores indicated better performance and log transformed) (Donohue et al., 2017, 2014). The PACC was constructed from available data in the sample. Components were z-transformed, summed and scaled to the baseline scores of the Aβ- CU.

Statistical analysis

The aims of these analyses were to (1) demonstrate the utility and predictive ability of the TFAβ+ formulation of Aβ information and (2) evaluate the relationship between TFAβ+ and CSF, PET, and cognitive responses in order to estimate the time of the earliest signs of progression. The overall analysis consisted of two steps. Step one was estimating TFAβ+ based on the longitudinal measures of global Aβ PET SUVR. In step two, TFAβ+ estimates were used to predict cross-sectional measures of regional tau and Aβ PET, CSF and cognitive outcomes. To demonstrate the value of the TFAβ+ measure, we did head-to-head comparisons of (i) TFAβ+ vs (ii) intercepts and slopes of longitudinal Aβ PET, modeled separately, to predict the outcomes. These comparisons are described in detail below.

Because TFAβ+ was not directly observed, in step one, linear mixed-effects models were fit to all available longitudinal global Aβ PET SUVR data to estimate subject-specific intercepts and slopes of Aβ pathology.

For the i^{th} individual at the j^{th} measurement time,

$$y_{ij} = \beta_0 + \beta_1 t_{ij} + b_{0i} + b_{1i} t_{ij} + e_{ij}, j = 1, \ldots, n_i,$$

where y_i is Aβ SUVR, β_0 and β_1 are the fixed intercept and slope over time, t_{ij} is time (years from baseline), b_{0i} and b_{1i} are the random intercept and slope over time, and e_{ij} is a Gaussian-distributed error term.

Because Aβ slopes are unlikely to remain constant over long periods of time as subjects move toward and away from the Aβ threshold, natural splines (Hastie and Tibshirani, 1990) were used to estimate the nonlinear shape of the slopes with respect to baseline Aβ, using quantile regression (Koenker and D'Orey, 1987). Rather than modeling the mean Aβ slope with respect to baseline Aβ, quantile regression provides a separate curve for each quantile, allowing the relationship between slope and intercept to differ depending on the location in the distribution of Aβ slope.

For a random variable X, with distribution function F, the τth quantile of X is defined as, $Q_X(\tau) = F^{-1}{}_X(\tau)$. Taking the sum of the random and fixed slope, $S_i = \beta_1 + b_{1i}$, gives subject-specific estimates of the slope over time of Aβ SUVR. Similarly, taking the sum, $I_i = \beta_0 + b_{0i}$, gives subject-specific estimates of the intercept of Aβ SUVR. Quantile curves were estimated by regressing S on I for $\tau \in (0, 1)$,

$$Q_{Si}(\tau) = \alpha_0(\tau) + \alpha_1(\tau) X_{1i} + \ldots + \alpha_k(\tau) X_{ki} + e_i,$$

where $x_{1i}, \ldots, x_{ki}$ is the k-dimensional natural spline basis for I_i. The dimension k, was selected by AIC.

For each subject, TFAβ+ was estimated by integrating over each subject's quantile curve from the subject's intercept to the threshold for Aβ-positivity (PET SUVR = 1.1). For example, for a subject with a baseline SUVR of 1.2 and a slope in the 0.6 quantile, TFAβ+ was taken to be the time it would take to go from SUVR = 1.1 to 1.2, using the slope estimates from the quantile curve. For incremental changes on the x-axis (baseline SUVR), the time required to travel the incremental distance is equal to distance/rate. Using the trapezoid rule (Atkinson, 1989), TFAβ+ is the sum of these incremental times spanning SUVR = 1.1–1.2. An example of calculating TFAβ+ is given in the top left panel of Fig. 1. Sensitivity analyses were done to determine the effect of varying the threshold for Aβ+. We repeated the estimation of TFAβ+ using an early threshold (SUVR 1.07) and a late threshold (SUVR 1.13).

To evaluate the accuracy of the TFAβ+ estimates, we compared the observed times of Aβ+ to the estimated times of Aβ+ values in participants who were Aβ- at baseline and became Aβ+ during follow-up. Observed time of Aβ+ occurred in the interval between the last Aβ- scan and the first Aβ+ scan. The observed time was calculated as a weighted average of the two scan times, weighted proportionally toward the scan where the participant was closest to hitting the threshold. Observed and estimated values were compared in $N = 37$ participants who crossed the threshold for Aβ+ and remained Aβ+ throughout follow-up. We also compared observed and estimated values in 44 participants including the original 37 plus seven additional subjects who crossed the threshold but had a subsequent negative scan.

Our analyses aim to model participants who are ostensibly on the AD trajectory and had calculable TFAβ+, i.e., they must be Aβ accumulators (positive rates of accumulation). Therefore, of the 982 participants with Aβ PET, we excluded $N = 20$ participants with negative Aβ accumulation rates (negative rates were largely driven by one early high Aβ PET measure), we also excluded $N = 6$ participants with low levels of Aβ and accumulation rates such that they were predicted to become Aβ+ later than 120 years of age (biomarker data from these subjects are included for visual comparisons in Figs. 3–5, see Figure legends). Fig. 1 shows the flow of participant inclusion. We included subjects where the TFAβ+ metric indicated very early accumulation of Aβ, but for participants estimated to have become Aβ+ before age 40 ($N = 25$, median estimated age at Aβ+ = 30, IQR: 27 to 34), we truncated TFAβ+ to age 40, based on previously described rates of Aβ-positivity in middle age (Jansen et al., 2015). These were mostly MCI and AD participants, *APOE* ε4 carriers, in their mid 60 s to late 70 s.

In the second step, the relationship between TFAβ+ and the responses was modeled using monotone penalized regression splines. The model takes the form,

$$y_i = f(\text{TFA}\beta+_i) + e_i = a_1(\text{TFA}\beta+_i)\beta_1 + \ldots + a_q(\text{TFA}\beta+_i)\beta_q + e_i,$$

where y_i is the one of the PET, CSF, or cognitive responses, measured cross-sectionally, and f is a smooth monotone function, represented by $a_1, \ldots, a_q$ basis functions. Generalized cross-validation was used to control the basis dimension q and the degree of smoothing (Wood, 1994). Cognitive responses were covaried for age, gender and education; CSF Aβ42, T-tau, P-tau and PET measures were covaried for age and gender.

Because the variance of the outcomes increases with advancing pathology and several outcomes contained clusters of extreme values, resulting in large residuals, we repeated step two of the analyses using M-estimation to provide robust estimates with robust standard errors (Huber and Ronchetti, 1981). This model takes the same form as described above, but is fit using iteratively reweighted least squares in order to downweight large residuals.

In order to account for the variance across steps 1 and 2, the entire process was repeated in 500 bootstrap samples to estimate 95% confidence intervals for the association between TFAβ+ and the responses.

To assess the predictive ability of TFAβ+, we compared (i) models using TFAβ+ vs (ii) models using both the subject-specific intercepts and slopes of longitudinal Aβ, to predict the responses. Two models for each response were compared. In model 1, responses were regressed on TFAβ+ using penalized regression splines as described above, adjusting for covariates. In model 2, responses were regressed on both Aβ intercepts and slopes using penalized regression splines, adjusting for covariates. Model 1 and 2 were compared using the Akaike Information Criterion (AIC) (Akaike, 1974).

Meaningful effect sizes of change of increase in pathology or decrease in cognition with respect to TFAβ+ were estimated as part of step two of the analysis. A Cohen's d effect size of 0.2 SD was considered small, 0.5 SD was considered medium, and a 0.8 SD effect was considered large (Cohen, 1988). A 0.2 standard deviation (SD) change from the mean response at the longest times (least pathological) from Aβ-positivity was taken to be the initial point of meaningful change. A 0.5 SD change was also shown as a more substantial effect size of change. For example, if the estimated mean PACC score at the lowest level of Aβ was 0 and the estimated mean PACC score at the time of Aβ-positivity was −0.5 and the residual SD of the PACC was 1.5, then the effect size at the time of Aβ-positivity = (−0.5 – 0)/1.5 = −0.33. A drop of 0.33 points on the PACC would be considered between a small (0.2) and medium (0.5) effect size, according to Cohen's guidelines for interpreting the magnitude of

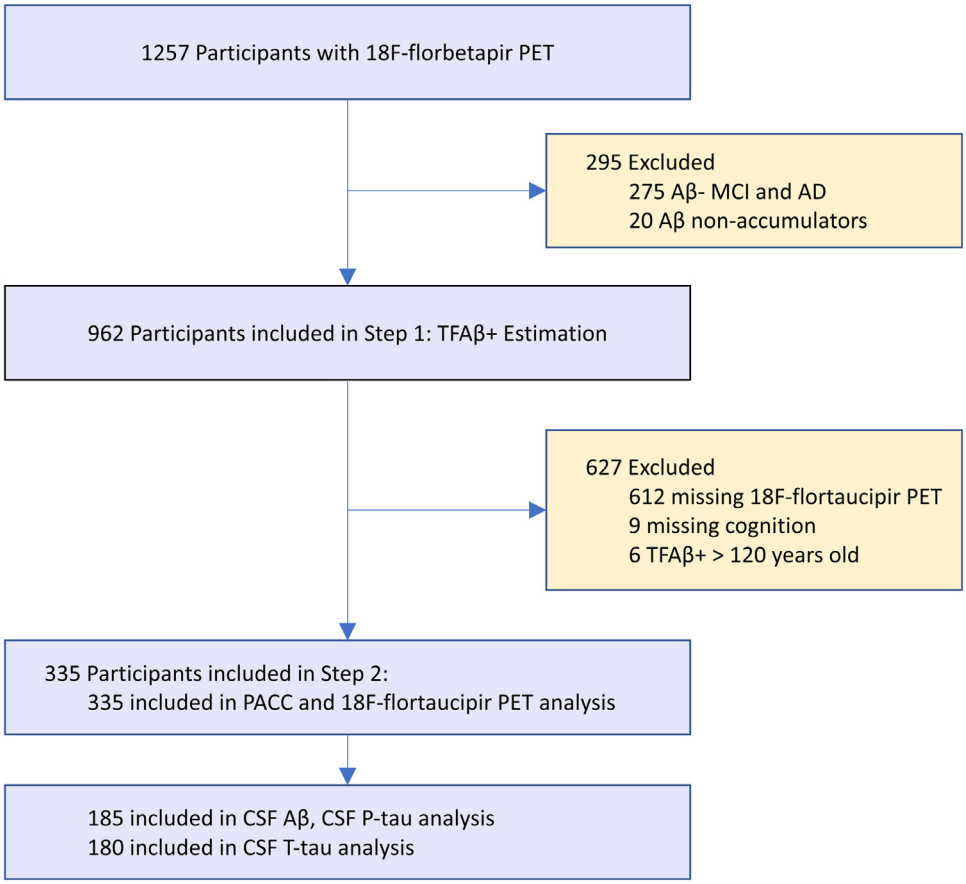

Fig. 1. Participant inclusion/exclusion.

Table 1
Cohort Characteristics.

	CU- (N = 127)	CU+ (N = 100)	MCI (N = 70)	AD (N = 38)	p
Age, mean (SD), y	70.1 (5.8)	72.9 (6.6)	72.0 (6.9)	74.5 (7.2)	<0.001
Sex, No. *F* (%)	76 (59.8)	58 (58.0)	29 (41.4)	18 (47.4)	0.06
Education, mean (SD), *y*	16.7 (2.4)	16.9 (2.3)	16.0 (2.7)	15.6 (2.5)	0.01
APOE ε4, No. carriers (%)	31 (25.6)	47 (50.5)	39 (60.9)	19 (54.3)	<0.001
TFAβ+, mean (SD), *y*	−8.9 (6.4)	13.8 (11.0)	20.9 (11.5)	25.5 (10.8)	<0.001

effect sizes. We also estimated change, 95% confidence intervals with bootstrap-estimated 2.5 and 97.5 quantiles, and statistical significance of change for each response at TFAβ+ = 0, the time of Aβ-positivity, with bootstrap-estimated standard errors.

Associations between missing data (CSF subsample vs full cohort) and demographics and TFAβ+ were evaluated using logistic regression with a binomial indicator for missing data. Baseline associations between demographics and TFAβ+ were assessed using Pearson correlation for age and years of education and a *t*-test for gender. Associations between diagnosis and demographics were assessed using F and t-tests for continuous variables and χ^2 tests for categorical variables. P-values were 2-sided and considered significant for $p < 0.05$. A drop of 2 or more in AIC was considered meaningful model improvement. All analyses were done in R v4.0.0 (www.r-project.org).

Results

Cohort characteristics

Two-hundred and twenty-seven CU (127 Aβ- and 100 Aβ+), 70 Aβ+ MCI and 38 Aβ+ AD participants were included in the analysis. The diagnostic groups varied by mean age, sex, years of education, and proportion of *APOE* ε4+ (Table 1). The CU- group was significantly younger than all other diagnostic groups ($p \leq 0.04$). The MCI group had a significantly smaller proportion of females than both the CU- group ($p = 0.02$) and the CU+ group ($p = 0.05$). The MCI group had significantly lower mean years of education compared to the CU- group ($p = 0.04$) and the CU+ group ($p = 0.02$). The AD group also had significantly lower mean years of education compared to the CU- group ($p = 0.01$) and the CU+ group ($p = 0.005$). The CU- group had a significantly smaller proportion of *APOE* ε4 carriers than all other diagnostic groups ($p<0.003$).

Aβ PET and estimation of TFAβ+

TFAβ+ was estimated with a median of 3 (range: 1 to 5) Aβ PET scans per participant. The average time between first and last scan was 3.3 years (SD=2.9) and the average time between scans was 2.2 years (SD=0.8). PET data came from 17 types of scanners across 58 sites. Neither site nor scanner type were associated with any Aβ PET outcome (ΔAIC > 12) or tau PET outcomes (ΔAIC > 19) and were not included in subsequent models. The correlation between subject-specific random intercepts and slopes was 0.32 (0.06 to 0.55). Residuals from the mixed model of repeated global Aβ PET SUVRs appeared approximately normal and with constant variance over time.

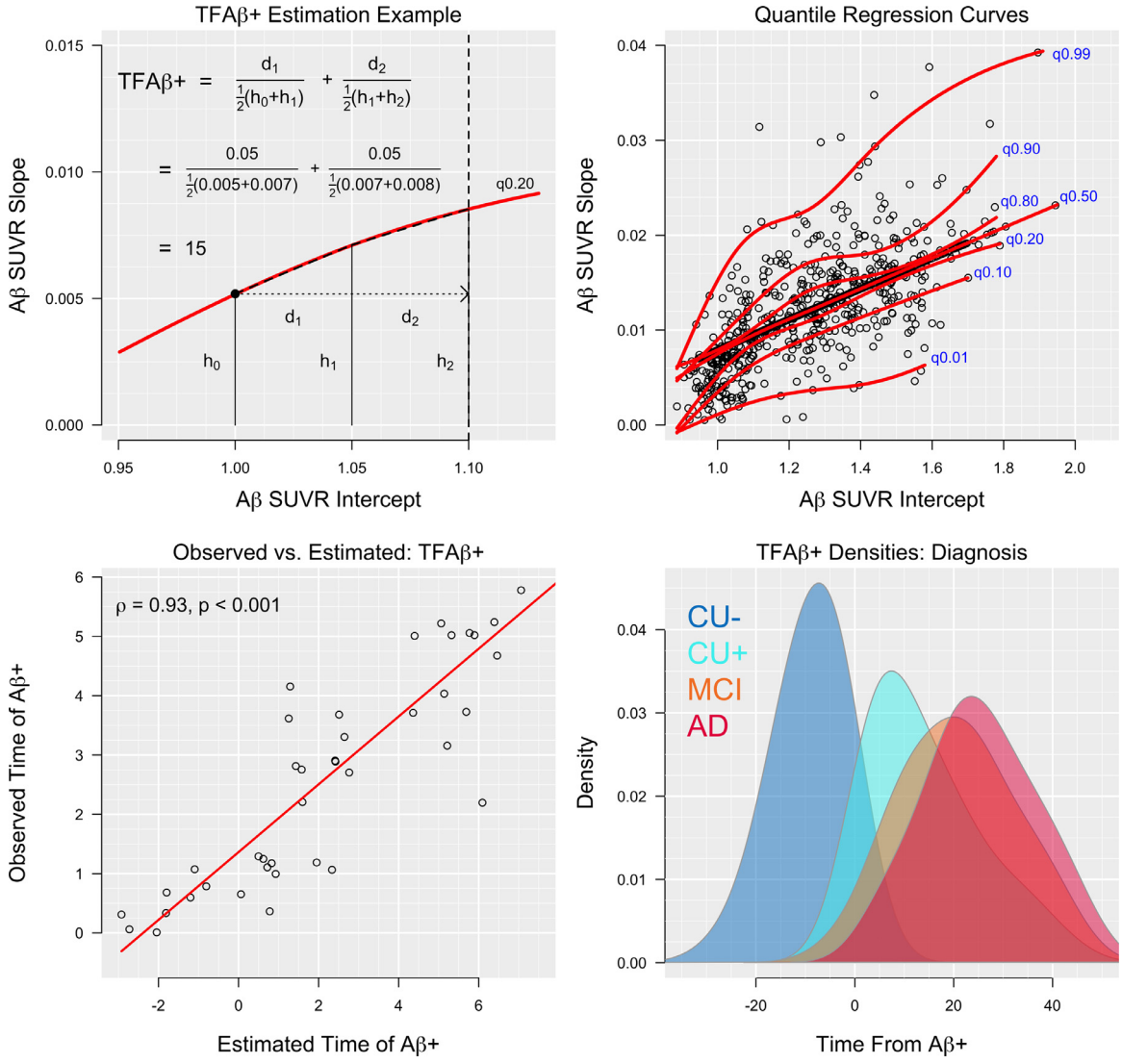

Fig. 2. Observed vs. estimated TFAβ+, quantile regression curves and TFAβ+ densities.
Top left panel: an example of how TFAβ+ is estimated. Here we have a participant with an estimated intercept of SUVR = 1.00 and an accumulation rate (slope) of 0.005 SUVR/year. We want to calculate how long it will take for them to reach the 1.10 threshold. A slope of 0.005 SUVR/year puts this participant on the 0.20 quantile (20% percentile) curve. We know this participant must accumulate 0.10 SUVR to reach the threshold and we will assume they will continue to have an accumulation rate in the 0.20 quantile. Partitioning the curve into segments from SUVR = 1.00–1.10 and using the formula time = distance/rate, the time to cross each segment is calculated and summed. In the figure, only two segments are shown, but in the actual calculation, the curve is partitioned into a large number of segments. Assuming a linear rate increase within each segment (shown in the dashed black line along the red quantile curve), the time to travel the distance in the 1st segment, from SUVR 1.00 to 1.05 is given by, $time_1 = d_1 / rate_1$, where d_1 is 0.05 and $rate_1$ is the average rate in segment 1, which is $\frac{1}{2}(h_0+h_1)$, as shown in the panel. A similar calculation is done for segment 2 and the results are summed to give TFAβ+ = 15.
Top right panel: quantile regression curves of Aβ PET slopes plotted against intercepts in all 962 participants with Aβ PET data. Curves for several selected quantiles (0.01, 0.10, …, 0.99) are shown in red.
Bottom left panel: observed time of Aβ+ plotted against estimated time of Aβ+ in the 37 participants who became and remained Aβ+ during follow-up.
Bottom right panel: distributions of TFAβ+ for each group, 127 Aβ- CU (CU-), 100 Aβ+ CU (CU+), 70 Aβ+ MCI, and 38 Aβ+ AD are shown.

Across diagnoses, TFAβ+ ranged from −29 to 46 years, where higher (positive) TFAβ+ values indicate more time spent with a significant Aβ burden. The CU- group had a significantly lower mean TFAβ+ compared to all other diagnostic groups (p<0.001). The CU+ group had a significantly lower mean TFAβ+ compared to the MCI group (p<0.001) and the AD group (p<0.001), and the MCI was significantly lower than the AD group (p = 0.02).

Higher TFAβ+ was significantly associated with older age (ρ=0.28, 95% CI: 0.17 to 0.37, p<0.001), lower education (ρ=−0.15, 95% CI: −0.25 to −0.04, p = 0.01) and *APOE* ε4-positivity (mean TFAβ+ in *APOE* ε4- = 3.3 (SD=16.1) years and mean TFAβ+ in *APOE* ε4+ = 13.6 (SD=15.8) years, p<0.001). TFAβ+ was not associated with sex (mean TFAβ+ = 9.4 (SD=17.1) and 6.8 (SD=16.4) in males and females, respectively, p = 0.16). Within-diagnosis TFAβ+ distributions are shown on the bottom right panel of Fig. 2. Quantile curves of the relationship between Aβ intercepts and slopes are also shown in the top right panel of Fig. 2, displaying the variation of acceleration of Aβ deposition over different levels of baseline Aβ.

TFAβ+ estimates were not sensitive to alternative thresholds for Aβ+ beyond a shift reflecting an earlier or later threshold. When the earlier threshold (SUVR 1.07) was used rather than SUVR 1.10, TFAβ+ estimates were shifted a median of 3.2 years earlier, but remained almost perfectly correlated with TFAB+ using the SUVR 1.10 threshold (ρ=0.996). Similarly, when the late threshold was used (SUVR 1.13),

TFAβ+ estimates shifter a median of 3.1 years later, but also remained almost perfectly correlated with TFAB+ using the SUVR 1.10 threshold (ρ=0.997).

TFAβ+ performance

TFAβ+ was highly correlated with observed time of Aβ+ (ρ=0.93, 95% CI: 0.87 to 0.97, p<0.001, bottom left panel of Fig. 2). When also including the seven participants with a subsequent negative scan after their initial positive scan, the correlation between TFAβ+ and the observed time of Aβ+ was 0.89, 95% CI: 0.80 to 0.94, p<0.001.

When comparing the performance of TFAβ+ versus using Aβ intercepts and slopes as separate predictors, TFAβ+ significantly outperformed separate intercepts and slopes most, but not all of the time. TFAβ+ significantly outperformed covariate only models for all outcomes. Using TFAβ+ resulted in significantly better prediction of MTL tau ($AIC_{TFA\beta+}$=345.1, $AIC_{IntSlope}$=360.2, AIC_{cov}=484.8), MPL tau ($AIC_{TFA\beta+}$=467.9, $AIC_{IntSlope}$=472.4, AIC_{cov}=532.9), occipital lobe tau ($AIC_{TFA\beta+}$=272.1, $AIC_{IntSlope}$=274.2, AIC_{cov}=325.8), CSF Aβ ($AIC_{TFA\beta+}$=1825.1, $AIC_{IntSlope}$=1827.4, AIC_{cov}=1962.1), CSF T-tau ($AIC_{TFA\beta+}$=1854.4, $AIC_{IntSlope}$=1863.4, AIC_{cov}=1902.9), MMSE ($AIC_{TFA\beta+}$=1534.8, $AIC_{IntSlope}$=1549.4, AIC_{cov}=1600.4), and the PACC ($AIC_{TFA\beta+}$=1251.2, $AIC_{IntSlope}$=1261.8, AIC_{cov}=1347.4). There was no difference between TFAβ+ and separate intercepts and slopes for LTL tau ($AIC_{TFA\beta+}$=398.6, $AIC_{IntSlope}$=399.5, AIC_{cov}=471.5) and CSF P-tau ($AIC_{TFA\beta+}$=1711.3, $AIC_{IntSlope}$=1709.6 AIC_{cov}=1748.3) and separate intercepts and slopes was significantly better than TFAβ+ in predicting frontal lobe tau ($AIC_{TFA\beta+}$=194.2, $AIC_{IntSlope}$=188.4, AIC_{cov}=245.9) and LPL tau ($AIC_{TFA\beta+}$=444.9, $AIC_{IntSlope}$=441.9, AIC_{cov}=512.3).

Regional Aβ PET

Five regional ROIs (precuneus + posterior cingulate, frontal lobe, cingulate gyrus, temporal and parietal lobes) are shown plotted against TFAβ+ in Fig. 3. All 5 regions were estimated to reach a small, but meaningful (0.2 SD) increase in SUVR between 12 and 15 years before Aβ-positivity, i.e. TFAβ+ = 0. Effect sizes over the span of TFAβ+ are shown in Fig. 3. At TFAβ+ = 0, all regions showed large, significant increases in SUVR (ΔSUVR $\geq$ 0.11, $p \leq 0.01$) with the precuneus + posterior cingulate composite showing the largest increase (ΔSUVR = 0.16, $p < 0.01$) and the temporal lobe showing the smallest (ΔSUVR = 0.11, $p < 0.01$). Effect sizes for all regions were large ($\geq$1) by the time of Aβ+. Table 2 summarizes the values of the outcomes at the longest times before Aβ+, i.e. the least pathological TFAβ+. Table 2 also shows the value and change of each outcome at the time of Aβ-positivity (TFAβ+ = 0), p-value, the effect size of change of each outcome, the 0.2 SD change point with respect to TFAβ+, and corresponding 95% confidence intervals.

Analyses of regional Aβ PET outcomes were repeated using robust regression with robust standard errors. The dashed blue curves in Fig. 3 depict the robust fit. The robust curves are similar to the unweighted regression curves with some mild flattening in the TFAβ+ = 5 to 25 year range. The 0.2 SD change point estimates for the increase in SUVR ranged from 18 to 20 years before Aβ-positivity (compared to 12–15 years before Aβ-positivity in the main analyses). Similar to the unweighted analyses, all regions showed significance of Aβ at TFAβ+ = 0 (p<0.01).

CSF

CSF responses are plotted against TFAβ+ in Fig. 4. A 0.2 SD drop in CSF Aβ42 was estimated to occur 29 years before Aβ-positivity (TFAβ+ = −29). At TFAβ+ = 0, CSF Aβ42 showed a very large effect size (ΔAβ42 = −68 ng/L, p<0.01, effect size = −1.99). At TFAβ+ = −2, or two years before Aβ-positivity, the population curve passes through a previously published CSF Aβ42 threshold for Aβ-positivity (192 ng/L) (Shaw et al., 2009).

A 0.2 SD increase in CSF T-tau and P-tau was estimated to occur 7–8 years before the time of Aβ-positivity (TFAβ+ = −7 and −8, respectively). At TFAβ+ = 0, significant increases of medium effect size of T-tau (ΔT-tau = 19 ng/L, p = 0.04, effect size = 0.46) and P-tau (ΔP-tau = 12 ng/L, p = 0.04, effect size = 0.47) were observed.

Robust curves are shown in dashed blue in Fig. 4. The change point estimate was 26 years before Aβ-positivity for the decrease in CSF Aβ, 13 years before Aβ-positivity for CSF P-tau, and 8 years before Aβ-positivity for CSF T-tau. A more substantial flattening of the curves can be seen in both CSF P-tau and T-tau for TFAβ+ > 0. The effect size for CSF T-tau at TFAβ+ = 0 remained almost identical (0.47, p = 0.03) and the effect size for CSF P-tau increased moderately to 0.56 (p = 0.01). The effect size for CSF Aβ42 increased to −2.52 at TFAβ+ = 0 and remained significant (p<0.01).

In comparing the CSF subsample (N = 185) to the full cohort, missing CSF Aβ42 (or P-tau) was not associated with age (OR=0.996, p = 0.42), sex (OR=1.08, p = 0.15), or TFAβ+ (OR=1.00, p = 0.96). Missing CSF T-tau was not associated with age (OR=0.996, p = 0.32), sex (OR=1.07, p = 0.22), or TFAβ+ (OR=1.00, p = 0.72).

Tau PET

Six regional ROIs (MTL, LTL, MPL, LPL, frontal and occipital lobes) are shown plotted against TFAβ+ in Fig. 5. Five of the six regions were estimated to reach a 0.2 SD increase in SUVR 3–5 years before Aβ-positivity, with the occipital lobe reaching a 0.2 SD increase at the time of Aβ-positivity. Effect sizes over the span of TFAβ+ are shown in Fig. 5. At TFAβ+ = 0, four regions (MTL, LTL, MPL, LPL) showed significant increases in SUVR (ΔSUVR $\geq$ 0.14, $p \leq 0.03$) with the MTL showing the largest effect size (0.36). The frontal and occipital lobes did not increase significantly by TFAβ+ = 0 (ΔSUVR = 0.09 (p = 0.06) and 0.07 (p = 0.13), respectively). Estimates are summarized in Table 2.

Robust curves are shown in dashed blue in Fig. 5. The robust curves show substantial flattening for TFAβ+ > 0. The robust 0.2 SD change point estimates for the increase in SUVR for the tau PET ROIs ranged from 6 to 9 years before Aβ-positivity. The significance of changes in tau PET at TFAβ+ = 0 were similar to the unweighted analyses with the exception of the frontal lobe, which increased in effect size and became statistically significant (0.44, p = 0.02).

Cognition

Cognitive measures are shown in Fig. 6. The MMSE showed a 0.2 SD drop six years before Aβ-positivity, followed by the PACC four years before Aβ-positivity. Neither measure decreased significantly by the time of Aβ-positivity (ΔMMSE = −0.71, p = 0.13, effect size=−0.30; ΔPACC = −0.50, p = 0.10, effect size=−0.32).

Robust curves are shown in dashed blue in Fig. 6 and show mild flattening for TFAβ+ > 0, compared to the unweighted analyses. The change point estimates for the decrease in cognitive scores was two years before Aβ-positivity for MMSE and four years before Aβ-positivity for the PACC. The robust estimate for the effect size of decrease in MMSE scores was reduced to −0.23 but became statistically significant (p = 0.03). The robust estimate for the effect size of decrease in PACC scores was similar (−0.30), and also became statistically significant (p = 0.03).

Summary curves and 0.2 SD change points for some of the earliest changing measures of each outcome type (CSF Aβ and P-tau, precuneus + posterior cingulate Aβ PET, MTL tau PET and the PACC) are shown in Fig. 7.

Discussion

Several biological processes develop over time in sporadic AD, including accumulation of Aβ and tau across wide areas of the brain, as well as cognitive decline. Based on the amyloid cascade hypothesis, a relevant overarching time scale of the disease processes could be based

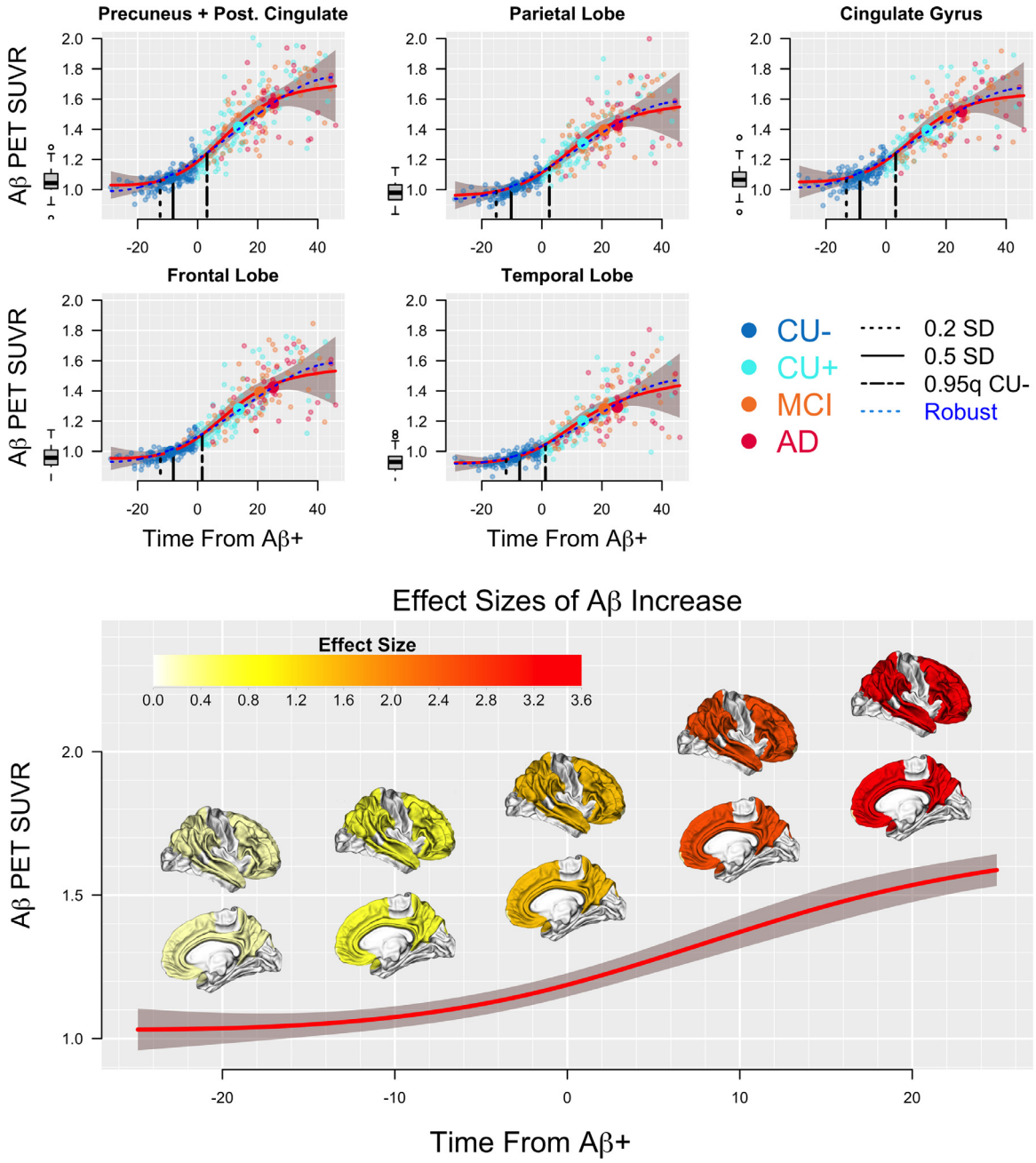

Fig. 3. Regional Aβ PET.
Aβ PET ROIs are plotted against TFAβ+. Effect sizes, depicting change points are shown as vertical dashed (0.2 SD, initial change) and solid (0.5 SD) lines. Unweighted regression curves (red) and corresponding 95% CIs (shaded gray) are shown. Robust curves are shown in dashed blue. Mean values of the response are plotted against mean TFAβ+ for each of the four diagnosis groups (large symbols). The 0.95 quantile (approximately 1.65 SD if normally distributed) of the response for the CU- group is also shown (short/long dashed line). The 0.95 quantile (or 0.05 quantile for responses where low values are worse) of the biomarkers in CU-, provided for all responses to facilitate comparisons of when (in terms of TFAβ+) the average level of each response is no longer in the normal range. The boxplots to the left of each figure show the biomarker distribution in subjects that were determined to not be on the AD trajectory (including subjects where the model estimated them to become Aβ+ at over 120 years of age). Effect sizes of Aβ increase are shown in the bottom panel at TFAβ+ = −20, −10, 0, 10, and 20 years.

on the development of Aβ pathology (Koscik et al., 2020). Integrating Aβ PET level and rate of change information places each individual on a pathological timeline. While this timeline, represented in these analyses by TFAβ+, was more closely associated with tau PET, CSF and measures of cognition in most measures, compared with intercept and slope information modeled separately, the main advantage is that it is parameterized to directly estimate the time of downstream events in the amyloid cascade. We estimated several major milestone events of AD progression including a small drop in CSF Aβ42 29 years before Aβ-positivity and a small increase in regional Aβ PET deposition 15 years before Aβ-positivity. Using the biomarkers tested here, the first changes in CSF Aβ42 may define the onset of AD. Small increases in tau pathology were estimated to occur 7–8 years before Aβ-positivity, as measured by CSF and 5 years before, as measured by PET. More substantial and statistically significant increases in CSF as well as temporoparietal tau PET were detected by the time of Aβ-positivity. Small effects of cognitive dysfunction occurred 4–6 years before Aβ-positivity, coinciding with previous reports (Insel et al., 2017). These findings provide a

Table 2
Initial values, effect sizes and change points.

	Initial value* (SD)	Value** at TFAβ+ = 0	Difference at TFAβ+ = 0 (p-value)	95% CI	Effect size (difference at TFAβ+ = 0)	95% CI	TFAβ+ Change Point (0.2 SD)	95% CI
Aβ PET (N = 335)								
Precuneus+PC	1.03 (0.14)	1.19	0.16 (<0.01)	0.06 to 0.25	1.10	0.43 to 1.79	−13	−21 to −5
Parietal Lobe	0.96 (0.12)	1.11	0.15 (<0.01)	0.06 to 0.24	1.20	0.50 to 2.00	−15	−23 to −8
Cingulate Gyrus	1.05 (0.13)	1.19	0.14 (0.01)	0.04 to 0.25	1.11	0.31 to 1.92	−13	−21 to −6
Frontal Lobe	0.95 (0.13)	1.09	0.14 (<0.01)	0.05 to 0.22	1.08	0.38 to 1.69	−12	−21 to −4
Temporal Lobe	0.92 (0.11)	1.03	0.11 (<0.01)	0.04 to 0.18	0.98	0.36 to 1.64	−12	−21 to −3
CSF								
Aβ (N = 185)	255 (34)	186	−68 (<0.01)	−109 to −28	−1.99	−3.18 to −0.81	−29	−38 to −20
T-tau (N = 180)	50 (42)	69	19 (0.04)	1 to 38	0.46	0.03 to 0.89	−7	−20 to 6
P-tau (N = 185)	27 (25)	38	12 (0.04)	1 to 22	0.47	0.03 to 0.90	−8	−22 to 5
Tau PET (N = 335)								
MTL	1.21 (0.41)	1.36	0.15 (0.01)	0.04 to 0.26	0.36	0.10 to 0.63	−5	−14 to 4
MPL	1.22 (0.49)	1.38	0.16 (0.01)	0.04 to 0.29	0.34	0.08 to 0.59	−5	−14 to 4
LTL	1.39 (0.44)	1.52	0.13 (0.03)	0.02 to 0.24	0.29	0.05 to 0.55	−3	−12 to 6
LPL	1.37 (0.47)	1.51	0.14 (0.03)	0.01 to 0.27	0.30	0.02 to 0.57	−4	−13 to 6
Frontal Lobe	1.39 (0.32)	1.49	0.09 (0.06)	0.00 to 0.19	0.29	0.00 to 0.59	−3	−15 to 8
Occipital Lobe	1.43 (0.36)	1.50	0.07 (0.13)	−0.02 to 0.16	0.20	−0.06 to 0.44	0	−11 to 11
Cognition (N = 335)								
MMSE	29.3 (2.38)	28.6	−0.71 (0.13)	−1.62 to 0.21	−0.30	−0.68 to 0.09	−6	−23 to 11
PACC	0.04 (1.57)	−0.46	−0.50 (0.10)	−1.08 to 0.09	−0.32	−0.69 to 0.06	−4	−16 to 8

* Initial Value indicates the estimated mean of the outcome at the minimum TFAβ+ value.
** Value at TFAβ+ = 0 is the model-estimated outcome value of the population curve at TFAβ+ = 0.

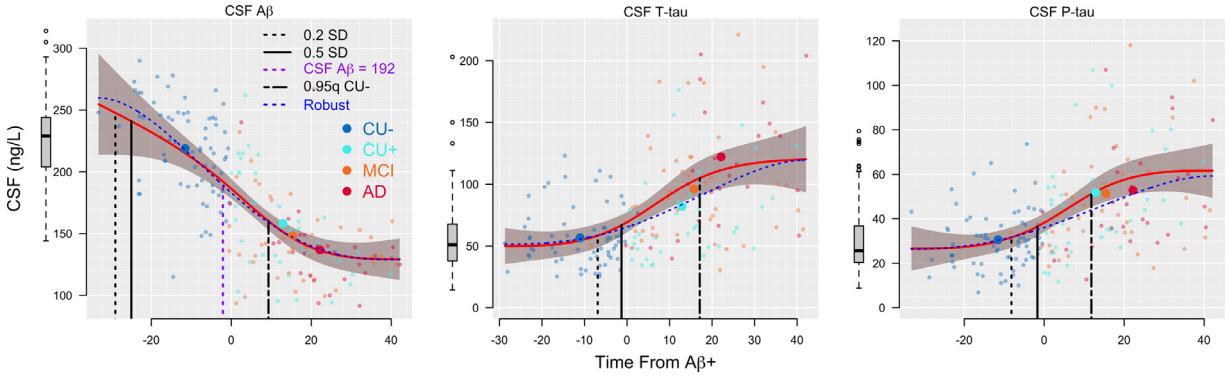

Fig. 4. CSF biomarkers.
CSF biomarker responses are plotted against TFAβ+. Effect sizes, depicting change points are shown as vertical dashed (0.2 SD, initial change) and solid (0.5 SD) lines. Un weighted regression curves (red) and corresponding 95% CIs (shaded gray) are shown. Robust curves are shown in dashed blue. Mean values of the response are plotted against mean TFAβ+ for each of the four diagnosis groups (large symbols). The 0.95 quantile (approximately 1.65 SD if normally distributed) of the response for the CU- group is also shown (short/long dashed line). The dashed purple line indicates a previously identified threshold for Aβ-positivity based on CSF Aβ. Note that this line occurs close to the TFAβ+ threshold for Aβ-positivity. The boxplots to the left of each figure show the biomarker distribution in subjects that were determined not to be on the AD trajectory (including subjects where the model estimated them to become Aβ+ over 120 years of age).

general time scale for initial changes in sporadic AD, which may inform clinical trials aimed at specific stages of the disease.

Once beyond the threshold for Aβ-positivity, there is a substantial increase in the variance of the tau and cognitive responses. A handful of participants show large increases, especially in tau PET, and large decreases in cognition, resulting in clusters of outliers. These outliers appear to have marked influence on both the shape of the curves and the estimates of the variance, as shown by the difference between the unweighted and the robust analyses. The robust curves are generally flatter beyond the threshold for Aβ-positivity, less influenced by extreme values. The curves are reasonably similar prior to Aβ-positivity, although the overall variance estimates are smaller, resulting in earlier estimates of change points for several of the outcomes and more significant differences at the threshold for Aβ-positivity. In both sets of analyses, significant increases in both CSF tau and tau PET are observed to occur by the time of Aβ-positivity.

A 0.2 SD difference, a small, but meaningful increase in levels of CSF tau and temporoparietal lobe tau are observed years before the current threshold for Aβ-positivity. In the context of secondary prevention trials where Aβ-positivity at current thresholds is required for study inclusion, tau levels in these participants would already have been increasing for several years, likely more. The finding that temporoparietal tau starts to increase prior to other regions is in accordance with 18F-flortaucipir studies on other populations. Cross-sectional studies showed early tau deposition in cognitively healthy elderly (with or without significant Aβ pathology) in temporal and medial parietal regions, most dominant in entorhinal and parahippocampal cortex, the amygdala and inferior temporal cortex. Longitudinal studies further suggest that cognitively healthy elderly accumulate tau in the medial temporal and medial parietal lobe, while (Aβ positive) AD dementia patients increased in tau primarily in the frontal lobe (Harrison et al., 2018). The spread of tau beyond the MTL to the parietal lobe and other regions may be a critical milestone in the progression of AD. The early changes observed in the MPL in this study coincide with a recent report of the earliest tau deposition found in medial parietal regions (precuneus and isthmus cingulate) in autosomal dominant AD (Gordon et al., 2019). Considering that a 0.2 SD increase in MPL tau can potentially be detected several years before Aβ-positivity (Fig. 5), these data support the use of primary

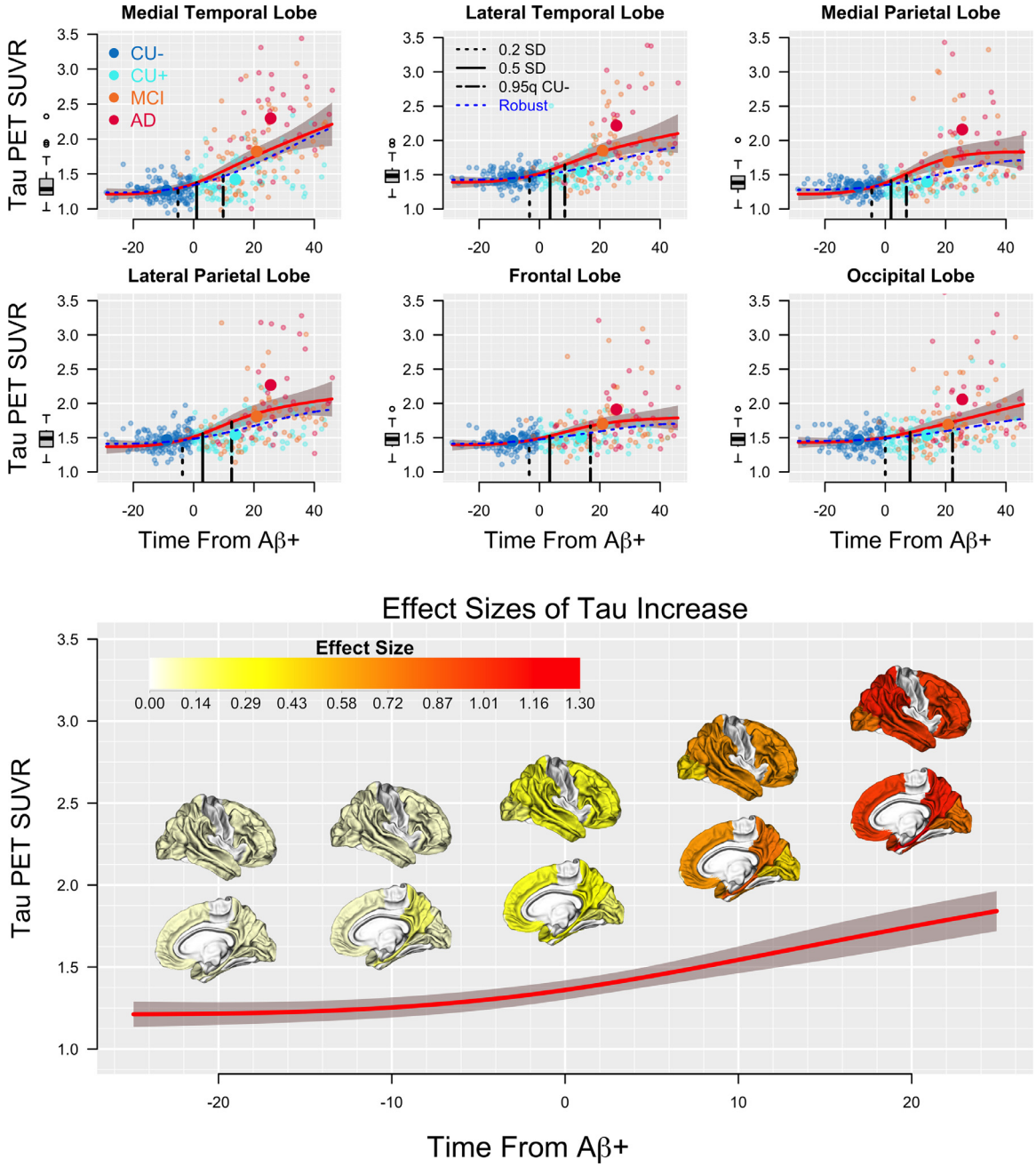

Fig. 5. Regional Tau PET.
Tau PET ROIs are plotted against TFAβ+. Effect sizes, depicting change points are shown as vertical dashed (0.2 SD, initial change) and solid (0.5 SD) lines. Unweighted regression curves (red) and corresponding 95% CIs (shaded gray) are shown. Robust curves are shown in dashed blue. Mean values of the response are plotted against mean TFAβ+ for each of the four diagnosis groups (large symbols). The 0.95 quantile (approximately 1.65 SD if normally distributed) of the response for the CU-group is also shown (short/long dashed line). The boxplots to the left of each figure show the biomarker distribution in subjects that was determined to not be on the AD trajectory (including subjects where the model estimated them to become Aβ+ at over 120 years of age). Effect sizes of tau increase are shown in the bottom panel at TFAβ+ = −20, −10, 0, 10, and 20 years.

prevention trials against Aβ where treatment is initiated years before the current threshold for Aβ-positivity, if treatment efficacy relies on early intervention, prior to the development of tau pathology.

The initial descent in cognitive performance is estimated to occur 4–6 years before becoming Aβ+ (Fig. 6). Reduced cognitive performance has repeatedly been shown to be associated with elevated levels of Aβ (Baker et al., 2017; Donohue et al., 2017; Insel et al., 2017, 2016), even within the subthreshold range (Landau et al., 2018), in cognitively unimpaired individuals. The result that CSF tau measures started to change between regional Aβ and cognition in this study is in accordance with the theory that cognitive impairment in AD is caused primarily by tau pathology. This is also in line with other recent studies which show that cognitive impairment is more strongly related to accumulation of tau than to Aβ (Ossenkoppele et al., 2019), and that both tau and Aβ appear necessary for cognitive decline (Sperling et al., 2019). The ordering of the responses coincides with the magnitude of the effect sizes at the time of Aβ-positivity (Table 1), suggesting that initial changes in the responses continue to change in parallel through to the time of Aβ-positivity, without any major differences in acceleration.

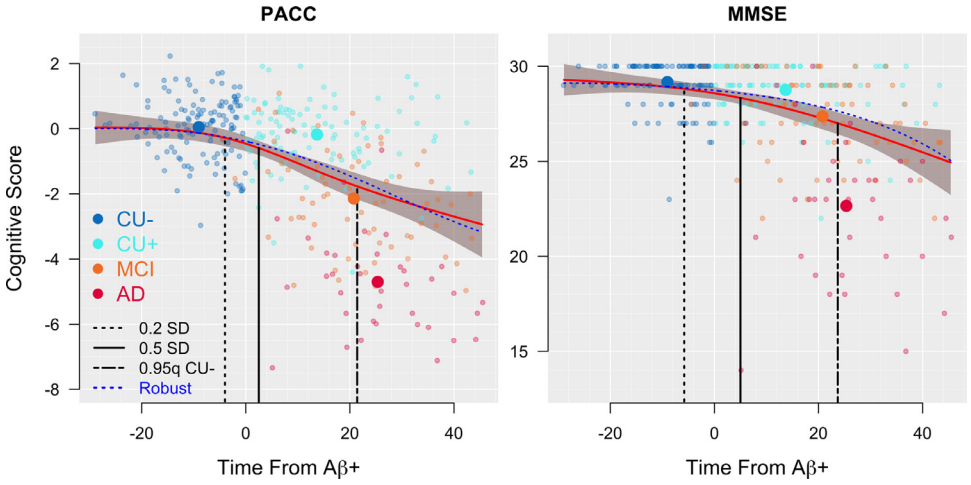

Fig. 6. Cognition.
MMSE and PACC scores are plotted against TFAβ+. Effect sizes, depicting change points are shown as vertical dashed (0.2 SD, initial change) and solid (0.5 SD) lines. Unweighted regression curves (red) and corresponding 95% CIs (shaded gray) are shown. Robust curves are shown in dashed blue. Mean values of the response are plotted against mean TFAβ+ for each of the four diagnosis groups (large ssymbols). The 0.05 quantile (approximately −1.65 SD if normally distributed) of the response for the CU- group is also shown (short/long dashed line). The overall PACC mean is −1.02 (SD=1.97).

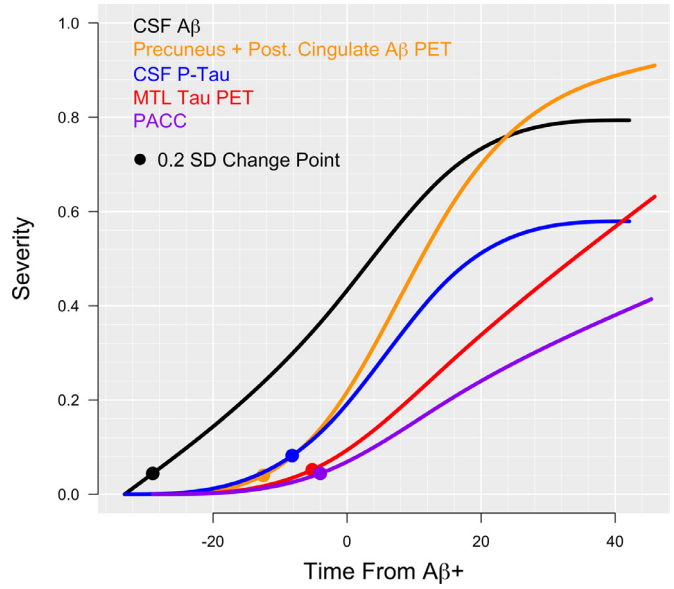

Fig. 7. Summary curves.
Summary curves are shown for all modalities on a scale from zero to one. Responses are scaled such that zero is the least pathological point for each response and one is the mean response in the AD participants. The initial effect, defined by 0.2 SD change points are plotted.

In their 2018 draft guidance, the FDA indicated that because it is highly desirable to intervene as early as possible in AD, it follows that patients with characteristic pathophysiologic changes of AD but no subjective complaint, functional impairment, or detectable abnormalities on sensitive neuropsychological measures are an important target for clinical trials (Food and Drug Administration, 2018). If the spread of tau to the lateral temporal and parietal lobes becomes a defining characteristic of pathophysiological change in AD, the window to intervene as early as possible may shift to years before the current threshold for Aβ-positivity. It is possible that early accelerations of tau may have contributed to recent failures of anti-Aβ treatments in phase III clinical trials on Aβ-positive patients (Egan et al., 2018; Honig et al., 2018). Although selecting subjects that are Aβ-positive ensures that only AD patients are included in trials, the use of conservative thresholds to define Aβ-positivity may bias trial populations toward individuals where tau pathology has already accumulated, causing downstream injuries independent of Aβ, reducing the efficacy of anti-Aβ treatments.

This study has several limitations. Tau PET data were available for only a subsample of the data, limiting comparisons to a small cross-section of the full ADNI data set. More data, especially longitudinal data in participants in the earliest stages of Aβ changes, will be required for more precise estimates of TFAβ+ as well as more precise change point estimates. Additional longitudinal Aβ information over longer periods of time will also be required to evaluate to what degree a participant may drift from their assumed quantile of accumulation. These analyses lack the power and precision to place the temporal and parietal tau regions in a particular order with confidence, but instead demonstrate that widespread tau is increasing years before Aβ-positivity. The ADNI CU, MCI and AD cohorts are also age matched. The AD patients, on average, have dementia by age 75, while the participants in the CU cohort who may eventually develop AD, are unlikely to do so for many years, possibly decades. By design, these cohorts with age matched groups are therefore on systematically different disease trajectories with respect to age. If earlier onset is associated with a more aggressive form of the disease, then the AD cohort may have the most aggressive form while the CU cohort, the least aggressive. If the developing Aβ pathology in the ADNI CU- cohort represents a less aggressive disease process compared with a more typical AD process, the estimates reported here could be conservative and biased toward later time estimates for downstream events. The ADNI MCI cohort may represent a more typical trajectory with respect to downstream events along the Aβ pathological timeline. These differences in disease trajectories are apparent from the cohort estimates in Figs. 2–5. Additionally, the change point estimates are influenced by both biological variation and measurement error, which varies from marker to marker. Change points in measures with high variability in the “normal” range and excess measurement error may require additional biological change to detect, despite an earlier, real increase in pathology. ADNI participants are highly educated on average, reducing generalizability to some degree. The associations between increasing Aβ pathology and downstream changes, including increased tau pathology reported here do not imply causality. It remains unknown whether and to what degree downstream pathological changes can be directly attributed to the accumulation of Aβ. Only studies with experimental interventions against Aβ-pathology, with clear verification of target engagement, can be used to show causal relationships between Aβ-deposition and putative downstream events. While TFAβ+ appears reasonably predictive, especially in proximity to the threshold for Aβ-positivity, longer follow-up is needed to validate its accuracy at very early and late-stage Aβ accumulation.

Longitudinal information is required to evaluate how quickly an individual’s pathophysiological changes are occurring and to accurately characterize their disease trajectory. Analyses limited to a cross-sectional evaluation of Aβ status are naïve to the time spent with a

significant Aβ burden. Incorporating longitudinal information facilitates the estimation of the time-course of downstream events such as the spread of tau and the onset of subtle cognitive dysfunction. As the technology to measure AD pathology becomes more cost effective and non-invasive, such as plasma measures of Aβ or tau (Janelidze et al., 2020; Mielke et al., 2018; Palmqvist et al., 2019; Schindler et al., 2019), longitudinal evaluations in the context of trial-ready cohorts may greatly improve early diagnosis and expedite the execution of clinical trials in early AD.

Data availability

All data is publicly available (http://adni.loni.usc.edu/). R code will be made available on Github.

Declaration of Competing Interest

Mr. Insel, Dr. Berron and Dr. Donohue report no competing interests.

Dr. Mattsson-Carlgren has been a consultant for ADNI.

Dr. Hansson has acquired research support (for the institution) from Roche, GE Healthcare, Biogen, AVID Radiopharmaceuticals and Euroimmun. In the past 2 years, he has received consultancy/speaker fees (paid to the institution) from Biogen and Roche.

Credit authorship contribution statement

Philip S. Insel: Conceptualization, Methodology, Software, Formal analysis, Writing - original draft, Writing - review & editing. **Michael C. Donohue:** Methodology, Writing - review & editing. **David Berron:** Methodology, Writing - review & editing. **Oskar Hansson:** Writing - review & editing, Funding acquisition. **Niklas Mattsson-Carlgren:** Methodology, Writing - review & editing, Funding acquisition.

Acknowledgments

Data collection and sharing for this project was funded by the Alzheimer's Disease Neuroimaging Initiative (ADNI) (National Institutes of Health Grant U01 AG024904). ADNI is funded by the National Institute on Aging, the National Institute of Biomedical Imaging and Bioengineering, and through generous contributions from the following: Alzheimer's Association; Alzheimer's Drug Discovery Foundation; BioClinica, Inc.; Biogen Idec Inc.; Bristol-Myers Squibb Company; Eisai Inc.; Elan Pharmaceuticals, Inc.; Eli Lilly and Company; F. Hoffmann-La Roche Ltd and its affiliated company Genentech, Inc.; GE Healthcare; Innogenetics, N.V.; IXICO Ltd.; Janssen Alzheimer Immunotherapy Research & Development, LLC.; Johnson & Johnson Pharmaceutical Research & Development LLC.; Medpace, Inc.; Merck & Co., Inc.; Meso Scale Diagnostics, LLC.; NeuroRx Research; Novartis Pharmaceuticals Corporation; Pfizer Inc.; Piramal Imaging; Servier; Synarc Inc.; and Takeda Pharmaceutical Company. The Canadian Institutes of Health Research is providing funds to support ADNI clinical sites in Canada. Private sector contributions are facilitated by the Foundation for the National Institutes of Health (www.fnih.org). The grantee organization is the Northern California Institute for Research and Education, and the study is coordinated by the Alzheimer's Therapeutic Research Institute at the University of Southern California, San Diego. ADNI data are disseminated by the Laboratory for Neuro Imaging at the University of Southern California. Data used in preparation of this article were obtained from the Alzheimer's Disease Neuroimaging Initiative (ADNI) database (adni.loni.usc.edu). As such, the investigators within the ADNI contributed to the design and implementation of ADNI and/or provided data but did not participate in analysis or writing of this report. A complete listing of ADNI investigators can be found at: http://adni.loni.usc.edu/wp-content/uploads/how_to_apply/ADNI_Acknowledgement_List.pdf.

This research was also supported by The Wallenberg Center for Molecular Medicine at Lund University, the Knut and Alice Wallenberg foundation, The Medical Faculty at Lund University, Region Skåne, the Skåne University Hospital Foundation, the Swedish Research Council, the Swedish Alzheimer Foundation, the Swedish Brain Foundation, the Swedish Medical Association, the Konung Gustaf V:s och Drottning Victorias Frimurarestiftelse, the Greta and Johan Kock Foundation, the Thelma Zoega Foundation, the Gyllenstiernska Krapperupsstiftelsen, the Magnus Bergwall Foundation, the Bundy Academy, the Marianne and Marcus Wallenberg foundation, and the Strategic Research Area MultiPark (Multidisciplinary Research in Parkinson's disease) at Lund University. The funding sources had no role in the design and conduct of the study, in the collection, analysis, interpretation of the data or in the preparation, review or approval of the manuscript.

References

ADNI, 2012. ADNI Commonly Used Tables [WWW Document]. URL https://adni.loni.usc.edu/wp-content/uploads/2012/08/instruction-about-data.pdf

Akaike, H., 1974. A new look at the statistical model identification. Autom. Control. IEEE Trans. 19, 716–723. doi:10.1007/s00198-008-0566-6.

Atkinson, K.E., 1989. An Introduction to Numerical Analysis, 2nd ed. John Wiley & Sons, New York.

Baker, J.E., Lim, Y.Y., Pietrzak, R.H., Hassenstab, J., Snyder, P.J., Masters, C.L., Maruff, P., 2017. Cognitive impairment and decline in cognitively normal older adults with high amyloid-β: a meta-analysis. Alzheimer's Dement. Diagnosis, Assess. Dis. Monit. 6, 108–121. doi:10.1016/j.dadm.2016.09.002.

Bateman, R.J., Xiong, C., Benzinger, T.L.S., Fagan, A.M., Goate, A., Fox, N.C., Marcus, D.S., Cairns, N.J., Xie, X., Blazey, T.M., Holtzman, D.M., Santacruz, A., Buckles, V., Oliver, A., Moulder, K., Aisen, P.S., Ghetti, B., Klunk, W.E., McDade, E., Martins, R.N., Masters, C.L., Mayeux, R., Ringman, J.M., Rossor, M.N., Schofield, P.R., Sperling, R.A., Salloway, S., Morris, J.C., 2012. Clinical and biomarker changes in dominantly inherited Alzheimer's disease. N. Engl. J. Med. 367, 795–804. doi:10.1056/NEJMoa1202753.

Braak, H., Braak, E., 1991. Acta H ' pathologica Neuropathological stageing of Alzheimer-related changes. Acta Neuropathol. 82, 239–259. doi:10.1007/BF00308809.

Cohen, J., 1988. Statistical Power Analysis for the Behavioral Sciences, 2nd ed. Lawrence Earlbaum Associates, New York.

Donohue, M.C., Sperling, R.A., Petersen, R., Sun, C.-K., Weiner, M.W., Aisen, P.S., 2017. Association between elevated brain amyloid and subsequent cognitive decline among cognitively normal persons. JAMA 317, 2305–2316. doi:10.1001/jama.2017.6669.

Donohue, M.C., Sperling, R.A., Salmon, D.P., Rentz, D.M., Raman, R., Thomas, R.G., Weiner, M., Aisen, P.S.Australian Imaging, Biomarkers, and Lifestyle Flagship Study of Ageing, Alzheimer's Disease Neuroimaging Initiative, Alzheimer's Disease Cooperative Study, 2014. The preclinical Alzheimer cognitive composite: measuring amyloid-related decline. JAMA Neurol. 71, 961–970. doi:10.1001/jamaneurol.2014.803.

Egan, M.F., Kost, J., Tariot, P.N., Aisen, P.S., Cummings, J.L., Vellas, B., Furtek, C., Harper Mozley, L., Mahoney, E., Vandenberghe, R., Mukai, Y., Voss, T., Mo, Y., Sur, C., Michelson, D., 2018. Randomized Trial of Verubecestat for Mild-to-Moderate Alzheimer's Disease. N. Engl. J. Med. 378, 1691–1703. doi:10.1056/nejmoa1706441.

Food and Drug Administration, 2018. Early Alzheimer's Disease: Developing Drugs for Treatment Guidance for Industry.

Gordon, B.A., Blazey, T.M., Christensen, J., Dincer, A., Flores, S., Keefe, S., Chen, C., Su, Y., Mcdade, E.M., Wang, G., Li, Y., Hassenstab, J., Aschenbrenner, A., Hornbeck, R., Jack, C.R., Ances, B.M., Berman, S.B., Brosch, J.R., Galasko, D., Gauthier, S., Lah, J.J., Masellis, M., Dyck, C.H.Van, Mintun, M.A., Klein, G., Ristic, S., Cairns, N.J., Marcus, D.S., Xiong, C., Holtzman, D.M., Raichle, M.E., Morris, J.C., Bateman, R.J., Benzinger, T.L.S., 2019. Tau PET in autosomal dominant Alzheimer's disease: relationship with cognition, dementia and other biomarkers. Brain J. Neurol. 142, 1063–1076. doi:10.1093/brain/awz019 BRAIN.

Hardy, J., Selkoe, D.J., 2002. The amyloid hypothesis of Alzheimer's disease: progress and problems on the road to therapeutics. Science 297, 353–356. doi:10.1126/science.1072994.

Harrison, T.M., La Joie, R., Maass, A., Baker, S.L., Swinnerton, K., Fenton, L., Mellinger, T.J., Edwards, L., Pham, J., Miller, B.L., Rabinovici, G.D., Jagust, W.J., 2018. Longitudinal tau accumulation and atrophy in aging and alzheimer disease. Ann. Neurol. 85, 229–240. doi:10.1002/ana.25406.

Hastie, T.J., Tibshirani, R.J., 1990. Generalized additive models. Monogr. Stat. Appl. Probab. doi:10.1016/j.csda.2010.05.004.

Honig, L.S., Vellas, B., Woodward, M., Boada, M., Bullock, R., Borrie, M., Hager, K., Andreasen, N., Scarpini, E., Liu-Seifert, H., Case, M., Dean, R.A., Hake, A., Sundell, K., Poole Hoffmann, V., Carlson, C., Khanna, R., Mintun, M., DeMattos, R., Selzler, K.J., Siemers, E., 2018. Trial of solanezumab for mild dementia due to Alzheimer's disease. N. Engl. J. Med. 378, 321–330. doi:10.1056/NEJMoa1705971.

Huber, P.J., Ronchetti, E.M., 1981. Robust Statistics. John Wiley & Sons, New York.

Insel, P.S., Donohue, M.C., Mackin, R.S., Aisen, P.S., Hansson, O., Weiner, M.W., Mattsson, N., 2016. Cognitive and functional changes associated with Aβ pathology and the progression to mild cognitive impairment. Neurobiol. Aging 48, 172–181. doi:10.1016/j.neurobiolaging.2016.08.017.

Insel, P.S., Ossenkoppele, R., Gessert, D., Jagust, W., Landau, S., Hansson, O., Weiner, M.W., Mattsson, N., 2017. Time to amyloid positivity and preclinical changes in brain metabolism, atrophy, and cognition: evidence for emerging amyloid pathology in alzheimer's disease. Front. Neurosci. 11, 1–9. doi:10.3389/fnins.2017.00281.

Jack, C.R., Knopman, D.S., Jagust, W.J., Shaw, L.M., Aisen, P.S., Weiner, M.W., Petersen, R.C., Trojanowski, J.Q., 2010. Hypothetical model of dynamic biomarkers of the Alzheimer's pathological cascade. Lancet Neurol. 9, 119–128. doi:10.1016/S1474-4422(09)70299-6.

Jagust, W.J., Landau, S.M., Koeppe, R.A., Reiman, E.M., Chen, K., Mathis, C.A., Price, J.C., Foster, N.L., Wang, A.Y., 2015. The Alzheimer's Disease Neuroimaging Initiative 2 PET Core: 2015. Alzheimer's Dement. 11, 757–771. doi:10.1016/j.jalz.2015.05.001.

Janelidze, S., Mattsson, N., Palmqvist, S., Smith, R., Beach, T.G., Serrano, G.E., Chai, X., Proctor, N.K., Eichenlaub, U., Zetterberg, H., Blennow, K., Reiman, E.M., Stomrud, E., Dage, J.L., Hansson, O., 2020. Plasma P-tau181 in Alzheimer's disease: relationship to other biomarkers, differential diagnosis, and longitudinal progression to Alzheimer's dementia. Nat. Med. 26, 379–386. doi:10.1038/s41591-020-0755-1.

Jansen, W.J., Ossenkoppele, R., Knol, D.L., Tijms, B.M., Scheltens, P., Verhey, F.R.J., Visser, P.J., Aalten, P., Aarsland, D., Alcolea, D., Alexander, M., Almdahl, I.S., Arnold, S.E., Baldeiras, I., Barthel, H., van Berckel, B.N.M., Bibeau, K., Blennow, K., Brooks, D.J., van Buchem, M.A., Camus, V., Cavedo, E., Chen, K., Chetelat, G., Cohen, A.D., Drzezga, A., Engelborghs, S., Fagan, A.M., Fladby, T., Fleisher, A.S., van der Flier, W.M., Ford, L., Förster, S., Fortea, J., Foskett, N., Frederiksen, K.S., Freund-Levi, Y., Frisoni, G.B., Froelich, L., Gabryelewicz, T., Gill, K.D., Gkatzima, O., Gómez-Tortosa, E., Gordon, M.F., Grimmer, T., Hampel, H., Hausner, L., Hellwig, S., Herukka, S.-K., Hildebrandt, H., Ishihara, L., Ivanoiu, A., Jagust, W.J., Johannsen, P., Kandimalla, R., Kapaki, E., Klimkowicz-Mrowiec, A., Klunk, W.E., Köhler, S., Koglin, N., Kornhuber, J., Kramberger, M.G., Van Laere, K., Landau, S.M., Lee, D.Y., de Leon, M., Lisetti, V., Lleó, A., Madsen, K., Maier, W., Marcusson, J., Mattsson, N., de Mendonça, A., Meulenbroek, O., Meyer, P.T., Mintun, M.A., Mok, V., Molinuevo, J.L., Møllergård, H.M., Morris, J.C., Mroczko, B., Van der Mussele, S., Na, D.L., Newberg, A., Nordberg, A., Nordlund, A., Novak, G.P., Paraskevas, G.P., Parnetti, L., Perera, G., Peters, O., Popp, J., Prabhakar, S., Rabinovici, G.D., Ramakers, I.H.G.B., Rami, L., Resende de Oliveira, C., Rinne, J.O., Rodrigue, K.M., Rodríguez-Rodríguez, E., Roe, C.M., Rot, U., Rowe, C.C., Rüther, E., Sabri, O., Sanchez-Juan, P., Santana, I., Sarazin, M., Schröder, J., Schütte, C., Seo, S.W., Soetewey, F., Soininen, H., Spiru, L., Struyfs, H., Teunissen, C.E., Tsolaki, M., Vandenberghe, R., Verbeek, M.M., Villemagne, V.L., Vos, S.J.B., van Waalwijk van Doorn, L.J.C., Waldemar, G., Wallin, A., Wallin, Å.K., Wiltfang, J., Wolk, D.A., Zboch, M., Zetterberg, H., 2015. Prevalence of cerebral amyloid pathology in persons without dementia: a meta-analysis. Jama 313, 1924–1938. doi:10.1001/jama.2015.4668.

Joshi, A.D., Pontecorvo, M.J., Clark, C.M., Carpenter, A.P., Jennings, D.L., Mintun, M.A., Adler, L.P., Burns, J.D., Saha, K., Sadowsky, C.H., Kovnat, K.D., Lowrey, M.J., Arora, A., Seibyl, J.P., Skovronsky, D.M., 2012. Performance characteristics of amyloid PET with florbetapir F 18 in patients with Alzheimer's disease and cognitively normal subjects. J. Nucl. Med. 53, 378–384. doi:10.2967/jnumed.111.090340.

Koenker, R., D'Orey, V., 1987. Algorithm AS 229 : computing regression quantiles author (s): roger W . Koenker and Vasco D ' Orey Source. J. R. Stat. Soc. Ser. C (Appl. Stat.) 36 (3), 383–393 Published by : Blackwell Publishing for the Royal S. J. R. Stat. Soc. Ser. C (Applied Stat. 36.

Koscik, R.L., Betthauser, T.J., Jonaitis, E.M., Allison, S.L., Clark, L.R., Hermann, B.P., Cody, K.A., Engle, J.W., Barnhart, T.E., Stone, C.K., Chin, N.A., Carlsson, C.M., Asthana, S., Christian, B.T., Johnson, S.C., 2020. Amyloid duration is associated with preclinical cognitive decline and tau PET. Alzheimer's Dement. Diagnosis, Assess. Dis. Monit. 12, 1–10. doi:10.1002/dad2.12007.

Landau, S., Jagust, W., 2015. Florbetapir Processing Methods [WWW Document]. URL https://adni.bitbucket.io/reference/docs/UCBERKELEYAV45/ADNI_AV45_Methods_JagustLab_06.25.15.pdf

Landau, S.M., Horng, A., Jagust, W.J., 2018. Memory decline accompanies subthreshold amyloid accumulation. Neurology doi:10.1212/WNL.0000000000005354.

Landau, S.M., Mintun, M.A., Joshi, A.D., Koeppe, R.A., Petersen, R.C., Aisen, P.S., Weiner, M.W., Jagust, W.J., 2012. Amyloid deposition, hypometabolism, and longitudinal cognitive decline. Ann. Neurol. 72, 578–586. doi:10.1002/ana.23650.

Li, D., Iddi, S., Thompson, W.K., Donohue, M.C., 2017. Bayesian latent time joint mixed effect models for multicohort longitudinal data. Stat. Methods Med. Res. 1–11. doi:10.1177/0962280217737566.

Maass, A., Landau, S., Horng, A., Lockhart, S.N., Rabinovici, G.D., Jagust, W.J., Baker, S.L., La Joie, R., 2017. Comparison of multiple tau-PET measures as biomarkers in aging and Alzheimer's disease. Neuroimage 157, 448–463. doi:10.1016/j.neuroimage.2017.05.058.

Mielke, M.M., Hagen, C.E., Xu, J., Chai, X., Vemuri, P., Lowe, V.J., Airey, D.C., Knopman, D.S., Roberts, R.O., Machulda, M.M., Jack, C.R., Petersen, R.C., Dage, J.L., 2018. Plasma phospho-tau181 increases with Alzheimer's disease clinical severity and is associated with tau- and amyloid-positron emission tomography. Alzheimer's Dement. 14, 989–997. doi:10.1016/j.jalz.2018.02.013.

Mormino, E.C., Kluth, J.T., Madison, C.M., Rabinovici, G.D., Baker, S.L., Miller, B.L., Koeppe, R.A., Mathis, C.A., Weiner, M.W., Jagust, W.J., 2009. Episodic memory loss is related to hippocampal-mediated β-amyloid deposition in elderly subjects. Brain 132, 1310–1323. doi:10.1093/brain/awn320.

Olsson, A., Vanderstichele, H., Andreasen, N., De Meyer, G., Wallin, A., Holmberg, B., Rosengren, L., Vanmechelen, E., Blennow, K., 2005. Simultaneous measurement of β-amyloid(1-42), total Tau, and phosphorylated Tau (Thr181) in cerebrospinal fluid by the xMAP technology. Clin. Chem. 51, 336–345. doi:10.1373/clinchem.2004.039347.

Ossenkoppele, R., Smith, R., Ohlsson, T., Strandberg, O., Mattsson, N., Insel, P.S., Palmqvist, S., Hansson, O., 2019. Associations between tau, Aβ, and cortical thickness with cognition in Alzheimer disease. Neurology 92, e601–e612. doi:10.1212/wnl.0000000000006875.

Palmqvist, S., Janelidze, S., Stomrud, E., Zetterberg, H., Karl, J., Zink, K., Bittner, T., Mattsson, N., Eichenlaub, U., Blennow, K., Hansson, O., 2019. Performance of fully automated plasma assays as screening tests for Alzheimer disease-related β-amyloid status. JAMA Neurol. 76, 1060–1069. doi:10.1001/jamaneurol.2019.1632.

Palmqvist, S., Mattsson, N., Hansson, O., 2016. Cerebrospinal fluid analysis detects cerebral amyloid-?? accumulation earlier than positron emission tomography. Brain 139, 1226–1236. doi:10.1093/brain/aww015.

Palmqvist, S., Schöll, M., Strandberg, O., Mattsson, N., Stomrud, E., Zetterberg, H., Blennow, K., Landau, S., Jagust, W., Hansson, O., 2017. Earliest accumulation of β-amyloid occurs within the default-mode network and concurrently affects brain connectivity. Nat. Commun. 8. doi:10.1038/s41467-017-01150-x.

Schindler, S.E., Bollinger, J.G., Ovod, V., Mawuenyega, K.G., Li, Y., Gordon, B.A., Holtzman, D.M., Morris, J.C., Benzinger, T.L.S., Xiong, C., Fagan, A.M., Bateman, R.J., 2019. High-precision plasma β-amyloid 42/40 predicts current and future brain amyloidosis. Neurology doi:10.1212/wnl.0000000000008081.

Schöll, M., Lockhart, S.N., Schonhaut, D.R., O'Neil, J.P., Janabi, M., Ossenkoppele, R., Baker, S.L., Vogel, J.W., Faria, J., Schwimmer, H.D., Rabinovici, G.D., Jagust, W.J., 2016. PET imaging of tau deposition in the aging human brain. Neuron 89, 971–982. doi:10.1016/j.neuron.2016.01.028.

Shaw, L.M., Vanderstichele, H., Knapik-Czajka, M., Clark, C.M., Aisen, P.S., Petersen, R.C., Blennow, K., Soares, H., Simon, A., Lewczuk, P., Dean, R., Siemers, E., Potter, W., Lee, V.M., Trojanowski, J.Q., 2009. Cerebrospinal fluid biomarker signature in Alzheimer's disease neuroimaging initiative subjects. Ann. Neurol. 65, 403–413. doi:10.1002/ana.21610.

Sperling, R.A., Mormino, E.C., Schultz, A.P., Betensky, R.A., Papp, K.V., Amariglio, R.E., Hanseeuw, B.J., Buckley, R., Chhatwal, J., Hedden, T., Marshall, G.A., Quiroz, Y.T., Donovan, N.J., Jackson, J., Gatchel, J.R., Rabin, J.S., Jacobs, H., Yang, H.S., Properzi, M., Kirn, D.R., Rentz, D.M., Johnson, K.A., 2019. The impact of amyloid-beta and tau on prospective cognitive decline in older individuals. Ann. Neurol. 85, 181–193. doi:10.1002/ana.25395.

Villemagne, V.L., Burnham, S., Bourgeat, P., Brown, B., Ellis, K.A., Salvado, O., Szoeke, C., Macaulay, S.L., Martins, R., Maruff, P., Ames, D., Rowe, C.C., Masters, C.L., 2013. Amyloid β deposition, neurodegeneration, and cognitive decline in sporadic Alzheimer's disease: a prospective cohort study. Lancet Neurol. 12, 357–367. doi:10.1016/S1474-4422(13)70044-9.

Wood, S.N., 1994. Monotonic smoothing splines fitted by cross validation. SIAM 15, 1126–1133. doi:10.1137/0915069.

Zetterberg, H., Mattsson, N., 2014. Understanding the cause of sporadic Alzheimer's disease. Expert Rev. Neurother. 14, 621–630. doi:10.1586/14737175.2014.915740.